

Phosphaalkenes with Inverse Electron Density: Electrochemistry, Electron Paramagnetic Resonance Spectra, and Density Functional Theory Calculations of Aminophosphaalkene Derivatives

Patrick Rosa,^{*,†} Cyril Gouverd,[†] Gérald Bernardinelli,[‡] Théo Berclaz,[†] and Michel Geoffroy^{*,†}

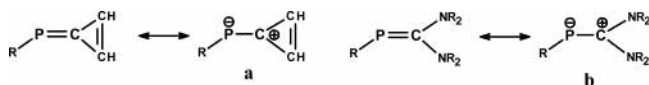
Department of Physical Chemistry, 30 Quai Ernest Ansermet, and Laboratory of Crystallography, 24 Quai Ernest Ansermet, University of Geneva, 1211 Geneva 4, Switzerland

Received: January 9, 2003

Cyclic voltammetry of Mes^{*}P=C(NMe₂)₂ (**1**) and Mes^{*}P=C(CH₃)NMe₂ (**2**) shows that, in solution in DME, these compounds are reversibly oxidized at 395 and 553 mV, respectively. Electrochemical oxidation or reaction of **1** (or **2**) with [Cp₂Fe]PF₆ leads to the formation of the corresponding radical cation, which was characterized by its electron paramagnetic resonance (EPR) spectra. Experimental ³¹P and ¹³C isotropic and anisotropic coupling constants agree with density functional theory (DFT) calculations showing that the unpaired electron is strongly localized on the phosphorus atom, in accord with the description Mes^{*}P[•]–(C(NMe₂)₂)⁺. Electrochemical reduction of **1** is essentially irreversible and leads to a radical species largely delocalized on the C(NMe₂)₂ moiety; this neutral radical results from the protonation of the phosphorus atom and corresponds to Mes^{*}(H)P[•]–C(NMe₂)₂. No paramagnetic species is obtained by reduction of **2**. The presence of the amino groups, responsible for the inverted electron distribution at the P–C double bond (P⁺–C[−]), confers on **1** and **2** redox properties that are in very sharp contrast with those observed for phosphaalkenes with a normal π electron distribution (P⁺–C[−]): no detection of the radical anion but easy formation of a rather persistent radical cation. For **1**, this radical cation could even be isolated as a powder, **1**^{•+}PF₆[−]. As shown by DFT calculations, this behavior is consistent with the decrease of the double bond character of the phosphorus–carbon bond caused by the presence of the amino groups.

1. Introduction

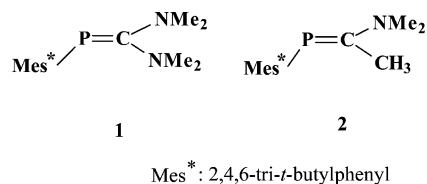
Phosphaalkenes have raised a great deal of interest in the last two decades for the similarities found between the P=C and the C=C bonds.^{1,2} Moreover, the presence of a low lying π* orbital confers to the P=C bond interesting electron acceptor properties that are easily demonstrated by the easy formation of radical anions and their detection by electron paramagnetic resonance (EPR) spectroscopy.³ Within this kind of compound, an especially interesting class was observed as early as 1986 by Regitz⁴ and by Grobe:⁵ whereas “common” phosphaalkenes are polarized in the sense P⁺–C[−], phosphatrifulvenes and C-amino substituted phosphaalkenes^{6–8} exhibit an inverted electron density.⁹ The corresponding mesomeric structures **a** and **b** suggest that the electron transfer behavior of such compounds



differs from that of “classical” phosphaalkenes and that both the formation and the electronic structure of the corresponding radical ions should be appreciably affected by this particular polarization.

As far as we know, no extensive study of the redox properties of these polarity-reversed phosphaalkenes has been made so far; the only indication to date is phenyl(1,3-dimesitylimidazolin-2-ylidene)phosphane,¹⁰ which shows an irreversible one-electron

oxidation wave at a potential value (−0.08 V vs SCE) that is appreciably inferior to those reported by Schoeller et al. for typical phosphaalkenes (1.07–2.94 V).¹¹ We decided, therefore, to study the cyclic voltammetry of two phosphaalkenes presenting all the properties associated with an inverse electron density, and to use EPR to identify their oxidation and reduction products. Two C-amino substituted phosphaalkenes were chosen for this purpose: the novel compound Mes^{*}P=C(NMe₂)₂ (**1**) and the phosphaalkene **2** whose synthesis has already been reported.¹²



The experimental hyperfine couplings are interpreted in terms of electronic configurations that are rationalized by density functional theory (DFT) calculations. It will be shown that the persistence of the radical species formed from these two compounds drastically differs from that observed with “classical” phosphaalkenes and that it is even possible, with **1**, to isolate the corresponding radical cation.

2. Results

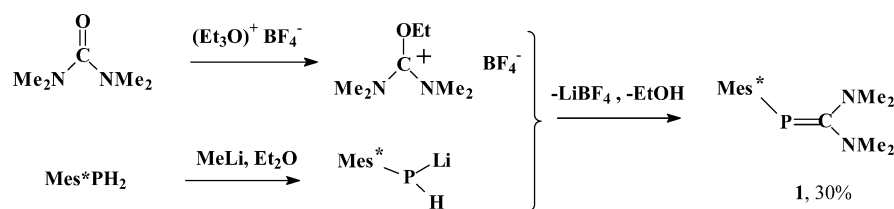
2.1. Synthesis and Chemical Properties. 2.1.a. Phosphaalkene 1. Phosphaalkene **1** was synthesized according to the method reported by Oehme et al.¹³ starting from easily available

[†] Department of Physical Chemistry.

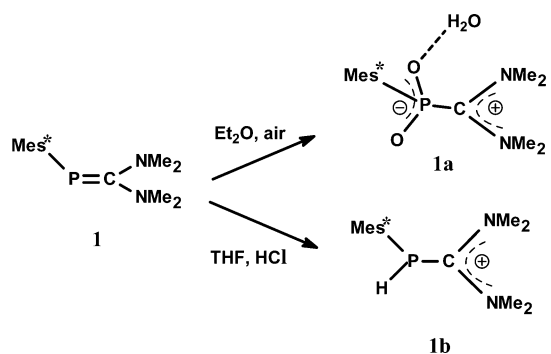
[‡] Laboratory of Crystallography.

* Corresponding author.

SCHEME 1

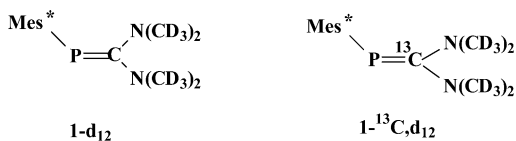


SCHEME 2



and relatively innocuous Mes^*PH_2 and bis(dimethylamino)-ethoxycarbenium tetrafluoroborate (Scheme 1).

Using the corresponding isotopically enriched ureas led to compounds $\mathbf{1-d}_{12}$ and $\mathbf{1-}^{13}\text{C},\text{d}_{12}$.



$\mathbf{1}$ is a yellow powder, easily handled in air, that is purified without any special precaution by silica gel chromatography. This stability is in marked contrast with usual phosphoranes that are sensitive toward oxygen and humidity. Unfortunately, crystals of X-ray diffraction quality could not be obtained.

The following NMR data confirm that \mathbf{b} represents a mesomeric form for $\mathbf{1}$ and are in accordance with values previously reported for other phosphoranes with reverse polarity. The ^{31}P NMR of $\mathbf{1}$ shows a resonance at $\delta = 28.3$ ppm, well upfield of usual phosphoranes (100–400 ppm),^{1,2,14} consistent with an increased electron density at the phosphorus atom. The ^{13}C NMR resonance at $\delta = 191.05$ ppm ($^1J_{\text{P-C}} = 76.90$ Hz) is typical of a sp^2 -hybridized carbon in a $\text{P}=\text{C}$ bond, while being quite downfield and in agreement with a strong cationic character. Last, both ^1H and ^{13}C NMR resonances of the dimethylamino groups distinguish *cis* and *trans* orientations relative to the phosphorus lone pair, as expected for a $\text{P}=\text{C}$ bond, but do not distinguish each methyl group attached to the nitrogen atoms, showing thus that for $\mathbf{1}$ free rotation around the C-N bonds occurs at room temperature.

As shown below, the reactivity of $\mathbf{1}$ (Scheme 2) is consistent with previous reports on inverse polarized phosphoranes and agrees with the expected electronic properties of this compound:

Reaction with Oxygen. When a solution of $\mathbf{1}$ in ether was left standing in contact with air, a very small quantity of white crystals was obtained after several weeks. The crystal structure of this compound was solved and showed that this oxidation product was the zwitterionic amidophosphinate $\mathbf{1a}$.¹⁵ This reaction (see Scheme 2) is similar to the reaction reported by Schmidpeter et al. for [bis(dimethylamino)methylene]phenylphosphane¹⁶ with ozone.

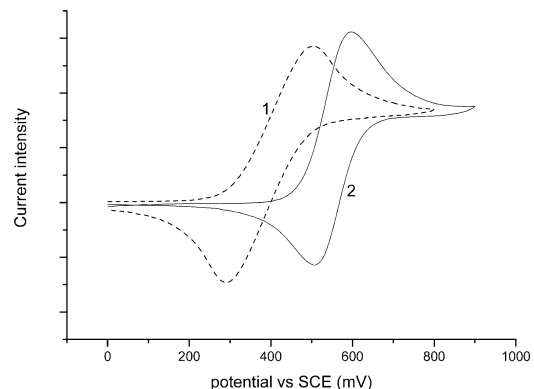


Figure 1. Cyclic voltammetry of the oxidation of a solution of $\mathbf{1}$ (···) in DME and of a solution of $\mathbf{2}$ in THF (—).

Reaction of Protonation. A solution of $\mathbf{1}$ in THF treated with gaseous HCl turned quickly colorless. ^{31}P NMR showed the unequivocal formation of a new compound at $\delta = -60.1$ ppm. Removal of the solvent yielded, quantitatively, a white powder that could be identified as the phosphinocarbenium chloride $\mathbf{1b}$ (Scheme 2). Protonation at phosphorus was visible in the ^1H NMR spectrum, with a resonance at $\delta = 6.20$ ppm ($^1J_{\text{P-H}} = 261.60$ Hz). This proton exchanges quickly with deuterium in the NMR time scale in acetone- d_3 . Monoprotonation was evidenced by the detection of the corresponding molecular ion by mass spectroscopy. ^1H and ^{13}C resonances of the two amino groups coalesce and are indistinguishable at room temperature. This shows a stronger delocalization of the nitrogen pairs over the $\text{C}(\text{NMe}_2)_2$ moiety compared to the parent compound and indicates that, in the protonated compound the rotation around the phosphorus–carbon bond is free. This agrees with protonation at phosphorus and disappearance of the double bond character of the phosphorus–carbon bond. These results are reminiscent of a previous report on $\text{RC}(\text{O})\text{P}=\text{C}(\text{NMe}_2)_2$.¹⁷

2.1.b. Phosphaalkene 2. Phosphaalkene $\mathbf{2}$ was synthesized according to the literature^{12,18,19} starting from Mes^*PH_2 and *N,N*-dimethylacetamide dimethyl acetal and was purified by silica gel chromatography.²⁰ The ^{31}P NMR shows a resonance at $\delta = 94.3$ ppm, closer to the values for “classical” phosphoranes, thus showing a decreased electron density at phosphorus compared with bis(amino) substituted $\mathbf{1}$. The ^{13}C NMR resonance of phosphorane carbon at $\delta = 189.2$ ppm ($^1J_{\text{P-C}} = 62.1$ Hz) concurs with this conclusion, showing a stronger $\text{P}=\text{C}$ bond.

2.2. Redox Properties. **2.2.a. Cyclic Voltammetry.** The voltammogram reported in Figure 1a shows that the oxidation of a solution of phosphorane $\mathbf{1}$ in DME occurs at $E_{1/2}^\circ = +395$ mV ($\Delta E_p = 218$ mV). A THF solution yields similar results ($E_{1/2}^\circ = +315$ mV, $\Delta E_p = 150$ mV). Variations of the current intensity with the scan rate indicate that this oxidation wave is reversible.

The reductive behavior of $\mathbf{1}$ is much less clear-cut. A nonreversible weak wave can be seen at $E_p \cong -800$ mV. Increasing the scan rate upward of 1 V/s reveals a return anodic

SCHEME 3

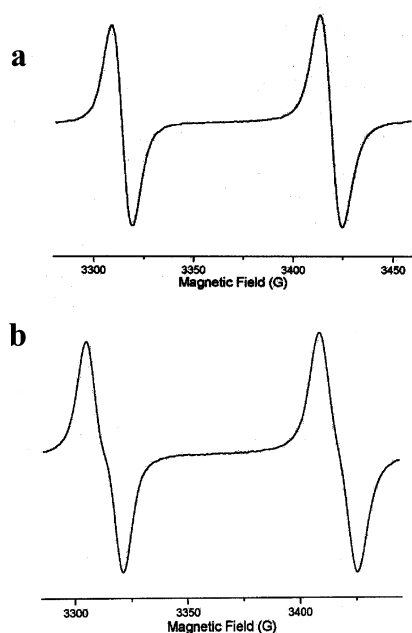
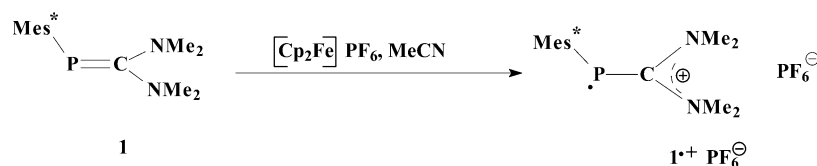


Figure 2. EPR spectra obtained at room temperature by electrochemical oxidation of (a) a solution of **1** in THF and (b) a solution of **1**-¹³C,_d12 in THF.

wave with an estimated $E^{\circ}_{1/2}$ value equal to -650 mV. This points to chemical irreversibility at low scan rates, very likely due to a protonation reaction of the radical anion. In this context, we have therefore carried out a voltammetric study of the phosphinocarbenium chloride **1b**. Two irreversible reduction waves were detected at $E_p = -610$ mV and $E_p = -970$ mV vs SCE.

Cyclic voltammetry (Figure 1b) indicates that a solution of **2** in THF undergoes an oxidation at $E^{\circ}_{1/2} = +525$ mV ($\Delta E_p = 205$ mV) (in DME: $E^{\circ}_{1/2} = +553$ mV, $\Delta E_p = 90$ mV). As shown by the variation of the current intensity with the scan rate, these oxidation waves are reversible. No reduction wave could be detected with **2**.

2.2.b. Chemical Oxidation. Chemical Oxidation of **1**. The easy electrochemical oxidation of **1** prompted us to attempt the synthesis of the corresponding radical cation by chemical oxidation. Adding 1 equiv of AgClO_4 in THF or $[\text{Cp}_2\text{Fe}]\text{PF}_6$ in acetonitrile to **1** results in the immediate formation of a deep violet solution, very sensitive to air. As shown by EPR (vide infra) the radical cation **1⁺•** is indeed formed in this reaction in accord with Scheme 3 and we could isolate the resulting salt.

The violet solid obtained after removal of the solvent can be kept for a few weeks in a glovebox if synthesized starting from $[\text{Cp}_2\text{Fe}]\text{PF}_6$. Unfortunately, we could not grow crystals suitable for X-ray diffraction. Stored under an inert atmosphere, a solution of **1⁺•PF₆⁻** will lose its color after a few days. The known oxidizing character of the perchlorate counteranion can account for the lesser stability of the compound when AgClO_4 is used in the synthesis.

Chemical Oxidation of 2. A solution of **2** in THF turns to pale yellow by addition of AgClO_4 but does not give rise to

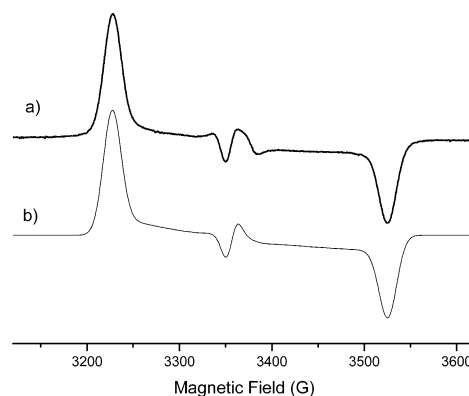


Figure 3. Frozen solution EPR spectra (120 K) obtained by electrochemical oxidation of **1**.

TABLE 1: Experimental EPR Parameters for the Oxidation Products of 1 and 2

precursor	liquid solution			frozen solution		
	g_{iso}	$A_{\text{iso}}(^{31}\text{P})$	$A_{\text{iso}}(^{13}\text{C})$	g	^{31}P -coupling (MHz)	
1	2.0077	296.2	23.8	$g_i = 2.0081$	$T_i = 1$	$\tau_i = -288$
				$g_j = 2.0136$	$T_j = 31$	$\tau_j = -258$
				$g_k = 2.0032$	$T_k = 835$	$\tau_k = 546$
				$g_{\text{av}} = 2.0083$	$A_{\text{av}} = 289$	
				$g_j = 2.0109$	$T_j = 46$	$\tau_j = -240$
2	2.0083	290.3	<i>a</i>	$g_i = 2.0114$	$T_i = 0$	$\tau_i = -286$
				$g_j = 2.0109$	$T_j = 46$	$\tau_j = -240$
				$g_k = 2.0035$	$T_k = 813$	$\tau_k = 527$
				$g_{\text{av}} = 2.0086$	$A_{\text{av}} = 286$	
				$g_j = 2.0109$	$T_j = 46$	$\tau_j = -240$

^a The ¹³C-enriched compound was not synthesized.

any EPR signal (vide infra). Oxidation with $[\text{Cp}_2\text{Fe}]\text{PF}_6$ is accompanied by a drastic change in the color of the solution, which progressively turns to deep red. The formation of the cation is detected by EPR (vide infra).

2.3. EPR Spectroscopy. **2.3.a. Oxidation Products.** At room temperature, electrochemical oxidation of a solution of **1** in THF, in situ in the EPR cavity, gives rise to the EPR spectrum shown in Figure 2. The same spectrum is obtained by directly oxidizing a THF solution of **1** with AgClO_4 in the EPR tube or by dissolving solid **1⁺•PF₆⁻** in carefully dried THF. In all cases, the color of the solution leading to the EPR spectrum is violet.

This spectrum consists of a doublet with a large splitting of ca. 295 MHz, which is attributed to hyperfine coupling with the ³¹P nucleus. The peak-to-peak line width is large, 10.5 G (1.05 mT), and points to other nonresolved hyperfine interactions. No significant shape alteration is seen upon cooling the solution till freezing temperature is reached. The frozen solution spectrum was recorded at 120 K and is shown in Figure 3a. As shown in Figure 3b, it was satisfactorily simulated by using a least-squares iterative procedure;²¹ the resulting g and ³¹P hyperfine tensors are found to be oriented parallel to each other. Assuming all the hyperfine components to be positive leads to an isotropic coupling constant in agreement with the isotropic constant measured in liquid solution.

The experimental EPR parameters are reported in Table 1.

The EPR spectrum obtained in liquid solution after oxidation of the ²H enriched phosphoalkene **1-d₁₂** is similar to the spectrum

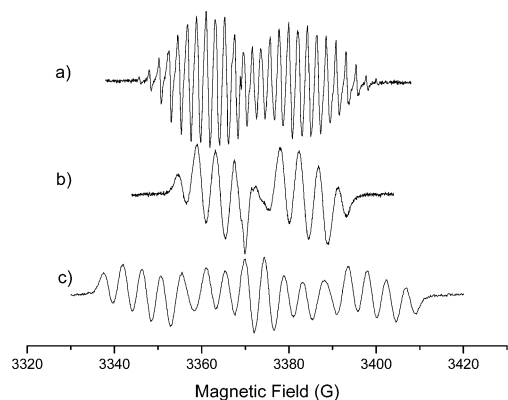


Figure 4. EPR spectra obtained by electrochemical reduction of a solution of (a) **1** in THF, (b) **1-d**₁₂ in THF, and (c) **1-¹³C,d**₁₂ in THF.

TABLE 2: Experimental EPR Parameters Obtained after Reduction of a Solution of **1 in THF**

precursor	<i>g</i>	isotropic hyperfine couplings (MHz)				
		³¹ P	¹ H	² H	¹⁴ N	¹³ C
1	2.0033	53.8 (×1)	6.17 (×12)		12.1 (×2)	
1-¹³C,d ₁₂	2.0033	53.8 (×1)		0.95 (×12)	12.1 (×2)	90.5 (×1)

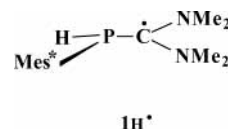
obtained with the nondeuterated compound, the single difference lies in a decrease of the line width to 8.7 G (0.87 mT), thus supporting the existence of non resolved hyperfine couplings with the dimethylamino protons. Nevertheless, the line width remains quite large and implies some interaction with the two ¹⁴N nuclei and/or some protons of the Mes* group. To measure the hyperfine coupling with the phosphalkene ¹³C, spectra were recorded after oxidation of **1-¹³C,d**₁₂. As shown in Figure 2b, on the resulting spectrum the ¹³C interaction is revealed by shoulders only, in line with a coupling of 24 MHz. The ¹³C enrichment does not cause significant modifications of the frozen solution.

No EPR spectra could be obtained by oxidation of **2** with AgClO₄. However, oxidation of a solution of **2** in acetonitrile with [Cp₂Fe]PF₆ or electrochemical oxidation of a solution of **2** in THF led to spectra that could be recorded in both liquid and frozen solutions. The corresponding parameters, obtained after simulation, are shown in Table 1.

2.3.b. Reduction Products. Whereas no EPR signal could be obtained by reduction of **1** over a potassium mirror or by reaction with a solution of sodium naphthalenide in THF, interesting spectra could be recorded when electrochemical reduction was carried out using the following conditions: (a) separation of the anodic and cathodic compartments by a porous frit to avoid the strong signal due to the diffusion of the radical cation **1^{•+}** and (b) use of THF that has not been thoroughly dried. No coloration of the solution is observed at the cathode, and the signals quickly disappear when the current is turned off. As shown in Figure 4, the spectrum obtained with **1** (Figure 4a) exhibits a very rich hyperfine structure, which is considerably simplified when the protons of the dimethylamino groups have been replaced by deuteriums (**1-d**₁₂, Figure 4b). An additional drastic modification of the spectrum is observed after ¹³C enrichment of the phosphalkene carbon (**1-¹³C,d**₁₂, Figure 4c): obviously, this nucleus gives rise to a large coupling constant of ≈90 MHz. Simulation²² of the three spectra reported in Figure 4 could be performed by assuming hyperfine coupling with one ³¹P, one ¹³C, and the protons of the four dimethylamino groups, as shown in Table 2.

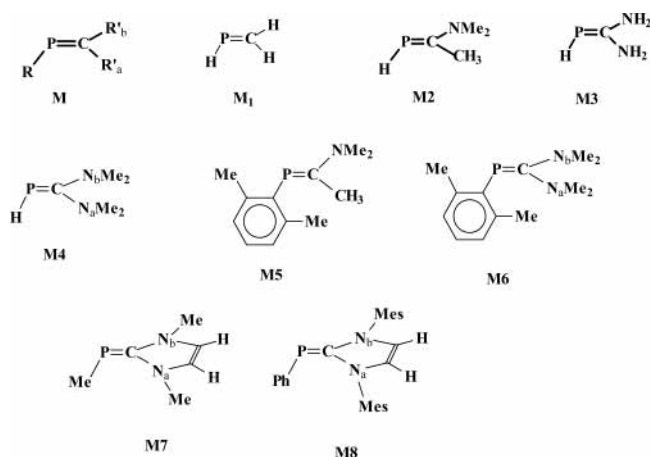
The fact that the spectra shown in Figure 4 are more easily detected when the solvent is not thoroughly dried prompted us

to investigate the effects of water on the spectra. Addition of 1 equiv of water resulted first in the disappearance of the signal; however, when electrolysis was resumed, the same spectrum was again observed with an increased intensity. Although no coupling with an additional proton is observed, this result suggests that the reduction products whose EPR spectra are shown in Figure 4 probably result from the protonation of the radical anion **1^{•-}** and correspond therefore to **1H[•]**.



Another mechanism can be invoked for the formation of this reduction compound: the reduction of trace amounts of phosphinocarbenium **1b** formed in a “wet” solution of phosphalkene **1**. To check this, we tried therefore to reduce phosphinocarbenium chloride **1b**, directly in the EPR cavity. Because the cyclic voltammogram of **1b** exhibits two close irreversible reduction waves, it was necessary to use a three-electrode EPR cell, which enables control of the applied potential. When a potential close to the first observed peak potential was applied, no EPR signal was observed. Decreasing the potential further by 300 mV did not give further results. It seems therefore that the EPR spectra result from the protonation of **1^{•-}**. No EPR spectra could be obtained by reduction of **2**.

2.4. DFT Calculations. With the aim of rationalizing the redox behavior of phosphalkenes containing NR₂ groups bound to the phosphalkene carbon atom, we have carried out DFT calculations on neutral RP=CR_aR_b model systems (**M**) as well



as on both radical anion and radical cation derivatives. The resulting structures will be compared with those recently reported on neutral [bis(amino)methylidene]phosphanes.^{7,8}

2.4.a. Neutral Phosphalkenes. As shown in Table 3, the geometric parameters obtained after optimization (B3LYP/6-31+G) of the phosphalkene models **M1–M8** are in satisfactory accord with the rare experimental data reported in the literature.

This table shows a progressive increase in both the experimental and DFT C=P bond lengths when the methylene hydrogens of phosphalkenes are substituted by NMe₂ groups (e.g., **M1, M2, M4** or **M5, M6**). This effect reflects the decrease in the double bond character of the phosphalkene bond and is reminiscent of recent results on model molecules whose phosphalkene carbon atom was incorporated in an imidazolynilidene structure.^{7,8} This decrease is illustrated by the consequent diminution of the rotation barrier²³ *V*_{rot} around the double bond: CH₂=CH₂ (*V*_{rot} = 97.2 kcal mol⁻¹), HP=CH₂ (**M1**, *V*_{rot}

TABLE 3: DFT Optimized Geometrical Parameters for Some Neutral Phosphaalkenes ($\Sigma\theta_N$ = Sum of the Bond Angles for N_a and N_b ; α : Angle between the Normals to the RPC and $R'_aCR'_b$ Planes)

compound RP=CR' _a R' _b	bond lengths (Å)				bond angles			interplane angle, α	sum of bond angles, $\Sigma\theta_N$
	P=C	R-P	C-R' _a	C-R' _b	RPC	PCR' _a	PCR' _b		
M1									
DFT	1.677	1.432	1.089	1.088	97.6	125.4	119.3	0	
exp	1.673(2)	1.420(6)			97.4(4)	124.4(8)	118.4(12)	0	
M2									
DFT	1.744	1.425	1.515	1.371	94.7	123.3	120.6	21.21	356.6 (N_b)
M3									
DFT	1.740	1.430	1.387	1.382	94.6	127.4	120.8	13.17	345.7 (N_a) 344.1 (N_b)
M4									
DFT	1.750	1.424	1.392	1.392	96.0	127.1	119.8	13.63	353.2 (N_a) 352.2 (N_b)
exp	1.740(1)	1.42(3)	1.348(4)	1.391(4)	103(1)	124.2(3)	121.6(3)	25.12	355.6(5) (N_a) 354.3(6) (N_b)
M5									
DFT	1.742	1.862	1.512	1.379	103.6	124.7	119.5	29.6	355.5 (N_b)
M6									
DFT	1.752	1.860	1.384	1.397	105.5	128.4	118.4	21.12	359.5 (N_a) 352.4 (N_b)
M7									
DFT	1.773	1.890	1.388	1.387	104.3	134.7	120.8	18.23	357.8 (N_a) 360 (N_b)

TABLE 4: Adiabatic Vertical Ionization Potentials Calculated by DFT (Experimental Values Given in Parentheses) and Oxidation Potentials

compound	IP ^v (eV)	E_p^{ox} (solvent) (V vs SCE)
C ₂ H ₄	10.49 (10.51) ²⁷	
H ₂ C=CHNH ₂	8.35 (8.2) ²⁸	
H ₂ C=C(NH ₂) ₂	7.91	
HP=CH ₂ (M1)	10.53 (10.3) ²⁹	
HP=C(NH ₂) ₂ (M3)	7.61	
HP=C(NMe ₂) ₂ (M4)	7.09 (7.26) ³⁰	
MeP=C(NH ₂) ₂	7.26	
MeP=C(NMe ₂) ₂	6.72	
PhP=C(NH ₂) ₂	7.09	
PhP=C(NMe ₂) ₂	6.53	
(Me ₂ C ₆ H ₃)P=C(Me)NMe ₂ (M5)	6.85	+0.63 (THF) for 2
(Me ₂ C ₆ H ₃)P=C(NMe ₂) ₂ (M6)	6.52	+0.39 (THF) for 1
M7	5.98	-0.08 (MeCN) for M8 ¹⁰

= 68.7 kcal mol⁻¹), to HP=C(NH₂)₂ (**M3**, $V_{\text{rot}} = 28.4$ kcal mol⁻¹) and HP=Imidazolinyldene ($V_{\text{rot}} = 13.2$ kcal mol⁻¹). This trend in the variation of V_{rot} agrees with the NMR data reported above (synthesis of **1**): the resonances of the *cis*- and *trans*-dimethylamino groups do not coalesce, whereas this is the case for the phosphaalkenes with a imidazolinyldene ring.^{24,25}

Because the formation of a radical cation of a phosphaalkene constitutes an important aspect of the present study, we have used DFT to calculate adiabatic vertical ionization potentials (IP^v) for several phosphaalkenes containing amino groups, DFT calculations yielding correct IP^vs for unsaturated molecules.²⁶ These values, together with those that we have calculated for some ethylene derivatives are given in Table 4 in the presence of experimental values when available. The agreement between calculated and experimental values is satisfactory. The expected trends are well reproduced, with substitution by electron-releasing amino groups sharply decreasing the IP^v: -2.6 eV for C=C and -2.9 eV for C=P. Alkylamino groups and more electron-releasing substituents at phosphorus further decrease the IP^v.

2.4.b. Oxidized Species. The structures of **M1**^{•+}, **M2**^{•+}, **M3**^{•+}, **M4**^{•+}, **M5**^{•+}, and **M6**^{•+} have been optimized and some resulting geometrical parameters are reported in Table 5. In these radical cations the phosphaalkene P-C bond as well as the two nitrogen

atoms are practically coplanar. As shown by Tables 3 and 5, oxidation increases the P-C bond length, moderately for HP=CH₂ (+0.04 Å) drastically for the amino substituted compounds (ca. +0.1 Å). Moreover, the distance between the phosphaalkene carbon and nitrogen atoms are shorter in the cation than in the neutral molecule. These bond lengths (1.34 Å), shorter than for a C(sp²)-N(sp²) single bond (1.355 Å), clearly reflect a strong conjugation in the C(NR₂)₂ moiety. Nevertheless, as seen in Table 5, the NR₂ planes do not coincide with the NCN plane and the angle φ formed by the normals to these two planes increases when NH₂ is replaced by NMe₂. Replacing NH₂ by NMe₂ also causes an increase in the dihedral angle α between the RPC and NCN planes; this shows that, as for the neutral molecule,³¹ nonnegligible steric interactions occur between the phosphorus and nitrogen substituents. As expected, oxidation of **M2** or **M5** hardly decreases the C-CH₃ bond length.

Comparison between experimental and calculated hyperfine interactions is certainly an efficient method for asserting the identification of a radical. However, in contrast with the dipolar interaction, the ³¹P Fermi contact interaction is frequently poorly calculated by DFT methods³²⁻³⁴ and can be appreciably affected by the choice of the basis set, specially when spin polarization effects are likely to occur. Taking some comments of Nguyen et al.³² into account, we have used three different basis set for the calculation of the ¹³C and ³¹P hyperfine constants for **M2**^{•+}, **M4**^{•+}, **M5**^{•+}, **M6**^{•+}. The results are shown in Table 6. They clearly indicate that, indeed, the IGLO-III³⁵ and TZVP³⁶ basis sets lead to isotropic ³¹P constants appreciably larger than those obtained with 6-31G(d).

2.4.c. Reduced Species. Because the reduction compound detected by EPR (vide supra) could result either from the radical anion [RP=C(NR'₂)₂]^{•-} or from the protonation of this anion, we have optimized the structure of four species: [HP=C(NMe₂)₂]^{•-} (**M4**^{•-}) and H₂P-•C(NMe₂)₂ (**M4H**), [(Me₂C₆H₃)P=C(NMe₂)₂]^{•-} (**M6**^{•-}), and (Me₂C₆H₃)HP-•C(NMe₂)₂ (**M6H**). The various hyperfine couplings have been calculated for these geometries and are given in Table 7.

3. Discussion

As shown in the previous section, two salient features characterize the electron transfer behavior of phosphalkenes

TABLE 5: DFT Optimized Geometrical Parameters for Some Phosphaalkene Radical Cations ($\Sigma\theta_N$ = Sum of the Bond Angles for N_a and N_b ; α = Angle between the Normals to the Planes RPC and $R'_aCR'_b$; φ = Angle between the Normals to the Planes N_aCN_b and CN_aC (or CN_bC))

compound RP=CR' _a R' _b	bond lengths (Å)				bond angles			interplane angle		sum of bond angles, $\Sigma\theta_N$
	P=C	R-P	C-R' _a	C-R' _b	RPC	PCR' _a	PCR' _b	α	φ	
M1⁺	1.721	1.428	1.095	1.093	99.3	121.3	121.9	36.33		
M2⁺	1.837	1.420	1.506	1.320	93.2	121.6	119.5	1.9 1.2	1.2	362.2
M3⁺	1.864	1.423	1.328	1.330	93.1	123.2	116.4	0.0 0.0	0.0	
M4⁺	1.875	1.423	1.343	1.343	94.0	121.4	117.2	32.03	26.8 (N_a) 23.4 (N_b)	359.3 (N_a) 359.5 (N_b)
M5⁺	1.836	1.807	1.507	1.321	104.7	120.6	119.8	37.44	1.9	
M6⁺	1.871	1.812	1.346	1.346	106.0	121.9	117.1	47.20	26.9 (N_a) 23.9 (N_b)	359.5 (N_a) 352.4 (N_b)

TABLE 6: Calculated (DFT) Hyperfine Couplings (MHz) for the Radical Cation M2⁺, M4⁺, M5⁺, M6⁺

	¹³ C coupling				³¹ P coupling			
	<i>A</i> _{iso}	dipole			<i>A</i> _{iso}	dipole		
M2⁺								
6-31+G(d)	-21.9	-9.8	3.6	6.3	110.2	510.6	-264.5	-246.1
IGLO-III	-25.4	-10.7	3.9	6.8	155.2	545.6	-282.0	-262.7
TZVP	-28.4	-10.6	4.0	6.6	187.3	557.4	-288.4	-268.9
M4⁺								
6-31+G(d)	-17.5	-3.2	1.5	1.7	119.3	562.1	-290.7	-271.4
IGLO-III	-20.5	-3.5	1.5	2.0	162.4	603.1	-312.5	-290.6
TZVP	-22.6	-3.4	1.5	1.9	204.4	615.9	-318.3	-297.6
M5⁺								
6-31+G(d)	-10.9	-5.4	-0.3	5.7	129.8	421.4	-217.7	-203.7
IGLO-III	-15.3	-5.6	-0.6	6.1	159.6	455.6	-236.6	-219.0
TZVP	-17.2	-5.7	-0.5	6.1	188.6	464.6	-240.0	
M6⁺								
6-31+G(d)	-9.6	3.4	-1.0	-2.4	137.7	461.7	-238.0	-223.7
IGLO-III	-13.2	3.8	-1.2	-2.6	170.6	500.2	-258.9	-241.2
TZVP	-14.5	3.7	-1.1	-2.6	203.1	510.0	-262.8	-247.2

containing one or two amino groups bound to the phosphaalkene carbon: the oxidation product is easily formed and readily observed by EPR whereas the reduction product leads to EPR signals that are either dramatically dependent upon the experimental conditions (e.g., **1**) or that remain undetectable (e.g., **2**). These results are in sharp contrast to those previously reported for phosphaalkenes with a phenyl group bound to the carbon atom:³ these “common” phosphaalkenes gave no response by oxidation but led to intense and well-resolved spectra by reduction. The origin of these differences in the redox properties will be examined below.

The first difference between the two types of phosphaalkenes lies in the double bond character of the phosphorus–carbon bond. The fact that this character considerably diminishes when NR₂ groups are bound to the carbon atom is clearly seen from DFT results (Table 3) and, of course, agrees with previous observations on other phosphalkenes with inverse electron density:⁹ the P–C bond length increases with the presence of amino groups, and this effect is accompanied by a decrease in the rotation barrier around the phosphorus–carbon bond.

As seen from a population analysis (NBO³⁷), the phosphorus participation to the P–C π orbital increases from 47.0% in HP=C(CH₂) to 60.4% in HP=C(NH₂)₂. This variation reveals a delocalization of the nitrogen electrons toward the carbon atom

and is consistent with the occupancy of each nitrogen lone pair, which is substantially less than two electrons (average values: 1.813 for HP=C(NH₂)₂, 1.739 for HP=C(NMe₂)₂). These properties correspond to those reported by Arduengo et al.²⁵ for the structure of carbene–phosphinidene adducts, which point out that in the adduct between dimesitylimidazolin-2-ylidene and phenylphosphinidene, the p π –p π double bond between these two moieties is not well developed.

Reduction of “common” phosphaalkenes lead to radical anions whose P=C π^* orbital accommodates the extra electron.³ The fact that, in phosphaalkenes with inverse polarization, the double bond character of the phosphorus–carbon bond diminishes does not favor, therefore, the formation of such radical anions and, indeed, chemical or electrochemical reduction of **2** does not lead to any EPR signal. For the reduction product of **1**, the spectrum is characterized by ³¹P and ¹³C isotropic couplings (*A*_{iso}(³¹P) = 58 MHz, *A*_{iso}(¹³C) = 90.5 MHz), which notably differ from those observed for the radical anion of Mes^{*}P=C(H)Ph (*A*_{iso}(³¹P) = 152 MHz, *A*_{iso}(¹³C) = 16 MHz).^{3a} As shown in Table 7, the corresponding EPR parameters are more in accordance with the formation of a carbon-centered radical ArP(H)– \dot{C} (NH₂)₂ resulting from the protonation of the radical anion. This interpretation agrees with the fact that traces of water increase the intensity of the spectrum. However, in contrast with the DFT predictions for **M6H**, no hyperfine interaction with the additional proton is observed on the spectrum. This can be due to the presence, in **1H⁺**, of the *tert*-butyl groups, which force the P–H bond to be oriented almost perpendicular to the plane containing the phosphaalkene carbon and the two nitrogen atoms. Because this proton coupling mainly results from hyperconjugation, it is expected to vary as cos² ξ , where ξ is the dihedral angle between the P–H bond and the magnetic carbon 2p π orbital. A rapid calculation on H₂P– \dot{C} (NMe₂)₂ shows that, indeed, for ξ = 75°, the coupling is close to zero.

The formation of a one-electron oxidation compound of phosphaalkenes **1** and **2** is particularly interesting because, as far as we know, **1⁺** is the first dicoordinated phosphorus radical cation to be isolated as a powder; moreover, radical cations derived from systems involving P=C bonds could never be detected, except with phosphaallenes,³⁸ a highly delocalized system. The hyperfine couplings given in Table 1 show that the oxidation products of **1** or **2** are characterized by axial ³¹P

TABLE 7: Hyperfine Couplings (MHz) Calculated for the Anionic and Neutral Species Likely To Result from the Reduction of Phosphaalkenes Containing Two Amino Substituents (DFT Calculations at the B3LYP/TZVP//B3LYP/6-31+G(d) Level)

	<i>A</i> _{iso} (³¹ P)	<i>A</i> _{iso} (¹³ C)	<i>A</i> _{iso} (¹⁴ N)		<i>A</i> _{iso} (¹ H (CH ₃))	<i>A</i> _{iso} (¹ H (P))
			¹⁴ N _a	¹⁴ N _b		
[HP=C(NMe ₂) ₂] ^{•-} (M4⁻)	26.8	135.3	-2.2	12.4	-0.36 to +5.16	
H ₂ P– \dot{C} (NMe ₂) ₂ (M4H)	69.2	99.8	15.3	15.9	0.22–13.06	23.7–139.6
[(Me ₂ C ₆ H ₃)P=C(NMe ₂) ₂] ^{•-} (M6⁻)	29.0	95.0	0.8	10.5	-0.11 to +5.77	
(Me ₂ C ₆ H ₃)HP– \dot{C} (NMe ₂) ₂ (M6H)	-28.0	86.5	13.7	18.7	1.0–9.0	80.8

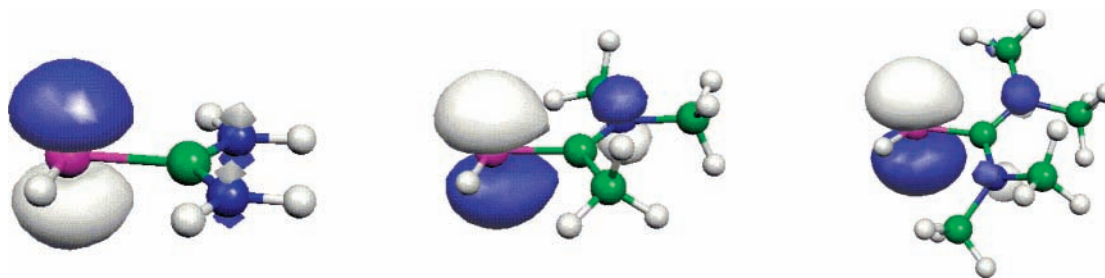


Figure 5. Representation of the SOMO for $\mathbf{M3}^+$, $\mathbf{M2}^+$, and $\mathbf{M4}^+$.

dipolar coupling tensors corresponding to a spin density of 0.75 in a phosphorus p orbital.³⁹ This strong localization of the unpaired electron induces an appreciable inner shell polarization, giving rise to an isotropic coupling constant that is quite higher than those observed with other radical species derived from phosphaalkenes. The absence of resolved dipolar coupling with ^{13}C together with the small $A_{\text{iso}}(^{13}\text{C})$ constant confirm that the unpaired electron is hardly delocalized on the phosphaalkene carbon. These properties, together with the fact that the axial \mathbf{g} -tensor is characterized by a g_{\parallel} value close to 2.0023 aligned along $^{31}\text{P}-\text{T}_{\parallel}$, are typical of a phosphinyl radical.⁴⁰ This result agrees with the DFT calculations (Tables 3 and 5), which indicate that the formation of the radical cation derived from $\text{RP}=\text{C}(\text{NH}_2)_2$ is accompanied by an elongation of the P–C bond, a shortening of the CN bonds (Tables 3 and 5) and a delocalization of the partial positive charge of the phosphaalkene carbon over the amino substituents. Indeed, natural population analysis³⁷ shows that electronic density loss at this carbon through oxidation is greatly diminished by amino substitution (carbon partial charges of $+0.28 e^-$ for $\mathbf{M1}$ to $+0.1 e^-$ for $\mathbf{M4}$), this diminution being concomitant with an enhanced donation of the nitrogen lone pairs (occupancy of $1.587 e^-$ in $\mathbf{M4}^+$). As shown by the SOMO of $\mathbf{M3}^+$ represented in Figure 5, the unpaired electron is localized in a phosphorus p_z orbital oriented perpendicular to the RPC plane, the corresponding phosphorus- p_z spin density is equal to $\rho = 0.87$ whereas the total spin density on the phosphorus atom is equal to 0.89 (for $\mathbf{M2}^+$ $\rho(\text{phosphorus-}p_z) = 0.79$, total phosphorus spin density 0.83; for $\mathbf{M4}^+$ $\rho(\text{phosphorus-}p_z) = 0.87$, total phosphorus spin density 0.91; for $\mathbf{M6}^+$ $\rho(\text{phosphorus-}p_z) = 0.69$, total phosphorus spin density 0.73).

Clearly, such a radical can be seen as a phosphinyl radical⁴⁰ bearing a stabilized carbenium group in the α position to the phosphorus atom (e.g. for $(\text{Et}_3\text{C}_6\text{H}_2)_2\text{P}^+$, $A_{\text{iso}}(^{31}\text{P}) = 275 \text{ MHz}^{40a}$). This identification and structure are confirmed by the good agreement between experimental (Table 1) and calculated (Table 6) hyperfine couplings. The electronic structures of these radical cations containing an amino group are quite different from the structure of cations derived from “classical” phosphaalkenes; e.g., for $(\text{HP}=\text{CH}_2)^+$ ($\mathbf{M1}^+$) the calculated spin density on the carbon atom ($\rho_{\text{C}} = 0.43$) is close to the spin density on the phosphorus atom ($\rho_{\text{P}} = 0.52$).⁴¹

Because inverse electron density seems to be involved in the ability of these phosphaalkenes to easily form persistent radical cations, it is worthwhile comparing the calculated vertical ionization potentials of several “common” phosphalkenes with those of phosphaalkenes with reverse polarity. As seen in Table 4, the expected trends are well reproduced, with substitution by electron-releasing amino groups decreasing the ionization potential values. Still more interesting in the context of electron transfer in solution, is the correlation between these vertical ionization potentials and irreversible electrochemical oxidation potentials. Schoeller et al. showed that a good correlation exists

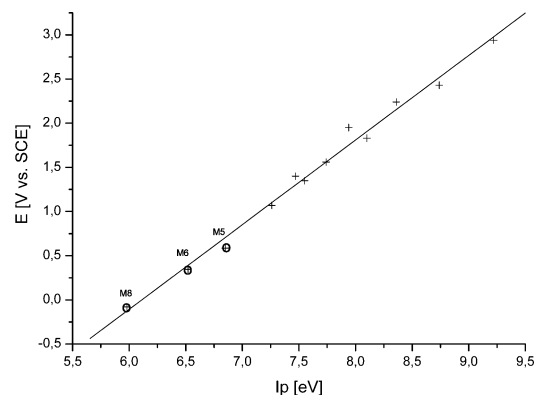


Figure 6. Correlation of experimental anodic potentials of phosphaalkenes with their vertical ionization potentials I_p . (The values of I_p are obtained from DFT calculations for $\mathbf{M5}$, $\mathbf{M6}$, and $\mathbf{M8}$ and from photoelectron spectroscopy for other compounds (This plot is an extension of the correlation reported by Schoeller et al.¹¹).

between these two values for “classically polarized” phosphaalkenes.¹¹

In Figure 6, we have reported the corresponding results together with those we have obtained for three phosphaalkenes with inverse electron density: $\mathbf{1}$, $\mathbf{2}$, and $\mathbf{M10}$ whose models are respectively $\mathbf{M6}$, $\mathbf{M5}$, and $\mathbf{M8}$. The data corresponding to these three last compounds beautifully fit those obtained by Schoeller et al.,¹¹ they extend the range of the correlation over 3 V and point out the relatively high facility of NR_2 -containing phosphaalkenes to form radical cations.

4. Conclusion

The electronic behavior of inversely polarized phosphaalkenes $\mathbf{1}$ and $\mathbf{2}$ has proved to be unexpectedly rich. Oxidation products $\mathbf{1}^+$ and $\mathbf{2}^+$ as well as a transient species $\mathbf{1H}^+$, resulting from protonation of $\mathbf{1}^+$, have been characterized. In contrast to radical cations derived from “classical” phosphaalkenes, $\mathbf{1}^+$ is easily available and stable. It may be said to behave as a stabilized analogue of transient phosphinyl radical. Further studies are now in progress concerning the coordination chemistry of these species and the electronic behavior of corresponding polyphosphaalkenes.

5. Experimental Section

Instrumentation. Cyclic voltammetry measurements were performed on a BAS station (model CV-50W), A standard three-electrode cell was used, with positive feedback IR compensation. All measurements were carried out under dry argon, The solution was made with 1,2-dimethoxyethane or THF, dried in a glovebox over activated 4 Å molecular sieves, as a solvent, NBu_4PF_6 (0.1 M), twice recrystallized and melt-dried under vacuum, as supporting electrolyte. A 1 mm diameter platinum wire as working and counter-electrode, and a SCE reference

electrode were used. The standard potential of ferrocene in THF is equal to 575 mV in our experimental conditions.

EPR spectra were recorded on a Bruker 200D spectrometer (X-band, 100 kHz field modulation) with a Bruker ER-4111 VT variable temperature controller. Samples were usually prepared by electrolysis in situ of a thoroughly argon degassed solution of the compound. A two platinum electrodes cell was used, the current intensity being adjusted till a signal appeared. For reduction experiments, the counter electrode was isolated from the working electrode by a small glass tube with a porous frit. For potential-controlled experiments, a three-electrode cell was used, with a 0.1 mm Ag wire treated with HCl/HNO₃ as pseudoreference. Full details for this cell will be published elsewhere. NBu₄PF₆ 0.1 M was again used as an electrolyte, with THF or DME as a solvent for the two-electrode cell, and CH₂Cl₂ for the three-electrode cell (THF does not allow a proper tuning of the EPR cavity).

NMR spectra were obtained on a Bruker 200AC and a Varian Gemini 200 spectrometers. All shifts are given in ppm, and coupling constants in Hz and referenced to internal solvent peaks or external 85% H₃PO₄. UV-vis spectra were obtained on a Varian Cary 50 Bio spectrometer.

Computation. Calculations were performed with the Gaussian 98 set of programs (G98).⁴² All geometries were optimized using the hybrid functional B3LYP,^{43,44} and the standard 6-31+G(d) basis set. Minima were characterized with harmonic frequency calculations (no imaginary frequencies). Zero-point energies thus calculated were corrected by a factor of 0.9804.⁴⁵ Natural population analysis was performed as implemented in Gaussian 98.⁴⁶ Molecular orbital visualizations were performed using the Molekel program.^{47,48} Ionization potentials were calculated as the electronic energy difference between ionized and neutral structure (with electronic relaxation but without structural relaxation), without ZPE correction. Proton affinities were calculated as the electronic energy difference between optimized protonated and neutral compound, with ZPE correction, neglecting other terms.^{49,50} Hyperfine coupling constants were calculated within the GIAO formalism implemented in Gaussian 98.⁵¹⁻⁵³

Syntheses. All syntheses were made using standard Schlenck line techniques under nitrogen atmosphere. Solvents were distilled over sodium before use. Mes*PH₂^{54,55} and bis(dimethylamino)ethoxycarbenium tetrafluoroborate⁵⁶ were synthesized according to literature procedures, CD₃I and ¹³C-labeled urea were purchased from Eurisotop. All other reagents were commercial.

(2,4,6-Tri-*tert*-butylphenyl)[bis(dimethylamino)methylidene]phosphane (**1**). In a dry Schlenck tube, 1.38 g of Mes*PH₂ (5 mmol) in 80 mL of ether was cooled to -80 °C. MeLi (1.6 M in ether, 3.13 mL) was syringed in the solution. The yellow solution was brought back to room temperature and then stirred for an additional h. The formation of the anion Mes*PHLi was then checked by ³¹P NMR.⁵⁴ The solution was then cooled to -50 °C, and bis(dimethylamino)ethoxycarbenium tetrafluoroborate (1.16 g, 5 mmol) was added. The mixture was brought slowly to room temperature over a couple of hours. ³¹P NMR showed peaks corresponding to the desired product and Mes*PH₂ (approximately 1/3 ratio). The product was purified by chromatography on silica gel, with hexane/ether 9:1 as an eluant, to obtain a pure yellow powder. Yield: 560 mg, 30%.

NMR (293 K): ³¹P (CDCl₃) δ 28.3; ¹H NMR (CD₂Cl₂) δ 1.28 (s, 9H, C_{para}-CMe₃), 1.55 (d, 18H, ⁵J(P-H) = 1.00, C_{ortho}-CMe₃), 2.16 (d, 6H, ⁴J(P-H) = 1.40, NMe₂), 2.79 (d, 6H, ⁴J(P-H) = 2.65, NMe₂), 7.25 (d, 2H, ⁴J(P-H) = 1.55,

H_{aromatic}); ¹³C (CDCl₃) δ 32.15 (s, C_{para}-CMe₃), 34.10 (d, ⁴J(P-C) = 8.65, C_{ortho}-CMe₃), 35.45 (s, C_{ortho}-CMe₃), 39.30 (s, C_{para}-CMe₃), 40.85 (s, NMe₂), 43.25 (d, ³J(P-C) = 18.60, NMe₂), 121.45 (s, C_{meta}), 138.45 (d, ¹J(P-C) = 59.95, C_{ipso}), 148.90 (s, C_{para}), 157.00 (s, C_{ortho}), 191.05 (d, ¹J(P-C) = 76.90, P=C). HRMS: calculated for ¹²C₂₃¹H₄₁¹⁴N₂³¹P 376.30074, measured 376.30200. Melting point: 93 °C. UV-vis (THF, nm): 245.1 (ε = 9.3 × 10⁵), 281.1 (7.7 × 10⁵), 307.0 (8.1 × 10⁵), 355.

*Tetramethylurea-d*₁₂. The synthesis was adapted from ref 57. In a 100 mL flask, DMSO (17 mL) was added to KOH powder (7.47 g, 133 mmol). The mixture was stirred for 10 min, and then urea (0.5 g, 8.33 mmol) was added. A condenser with a septum was then fit to the flask, the mixture was cooled with an ice-water bath, and then CD₃I (4.2 mL, 66.6 mmol) was added dropwise through the septum. The ice was then removed and replaced with cold water. After 1 h of stirring, the mixture was dissolved in 160 mL of distilled water and then extracted three times with 160 mL of dichloromethane portions. The resulting colorless solution was washed five times with 80 mL of distilled water portions and then dried over MgSO₄. The solvent was removed under water pump vacuum to give a colorless liquid. Yield: 0.34 g, 32%. The ¹³C-labeled urea was used in the same way to synthesize tetramethylurea-¹³C,*d*₁₂.

Corresponding labeled compounds **1-d**₁₂ and **1-¹³C**,*d*₁₂ were then synthesized as previously.

Overall yield starting from urea for **1-d**₁₂ and **1-¹³C**,*d*₁₂: 0.25 g, 8%.

For **1-d**₁₂: HRMS calculated for ¹²C₂₃¹H₂₉²H₁₂¹⁴N₂³¹P 388.37606, measured 388.37900.

For **1-¹³C**,*d*₁₂: NMR ³¹P (293 K, Et₂O) δ 35.5 (d, ¹J(P-¹³C) = 79.4). HRMS: calculated for ¹²C₂₂¹³C¹H₂₉²H₁₂¹⁴N₂³¹P 389.37941, measured 388.38200.

[(2,4,6-tri-*tert*-butylphenyl)phosphino]bis(dimethylamino)carbenium chloride (**3**). In a Schlenck tube, a solution of 75 mg of **1** in 5 mL of THF was exposed to gaseous HCl. The solution turned quickly colorless. Remaining HCl was then fluxed out with nitrogen, and the solvent was removed in vacuo to give a white powder. ³¹P NMR in dichloromethane showed the reaction to be quantitative.

NMR (293 K): ³¹P (CD₂Cl₂) δ -60.1; ¹H NMR (CD₂Cl₂) δ 1.31 (s, 9H, C_{para}-CMe₃), 1.51 (s 18H (C_{ortho}-CMe₃), 3.04 (broad s, 12H, NMe₂), 6.20 (d, 1H, ¹J(P-H) = 261.60, P-H), 7.49 (d, 2H, ⁴P-H) = 3.35, H_{aromatic}); ¹³C (CD₂Cl₂) δ 31.20 (s, C_{para}-CMe₃), 33.40 (d, ⁴J(P-C) = 6.60, C_{ortho}-CMe₃), 35.50 (s, C_{ortho}-CMe₃), 39.60 (s, C_{para}-CMe₃), 44.70 (broad s, NMe₂), 118.90 (d, ¹J(P-C) = 26.60, C_{ipso}), 124.20 (d, ³J(P-C) = 3.15, C_{meta}), 154.55 (s, C_{para}), 157.45 (d, ²J(P-C) = 9.95, C_{ortho}), 182.90 (d, ¹J(P-C) = 58.60, P-C). HRMS: calculated for ¹²C₂₃¹H₄₂¹⁴N₂³¹P⁺ 377.30856, measured 377.30540.

[(2,4,6-Tri-*tert*-butyldeuteriophenyl)phosphino]bis(dimethylamino)carbenium chloride. When product **3** was dissolved in acetone-*d*₆, ³¹P NMR did not show any spectrum. After removal of the acetone and addition of dichloromethane, ³¹P NMR showed the formation of the deuterated product. NMR (293 K): ³¹P (CH₂Cl₂) δ -61.1 (t, ¹J(P-²H) = 39.6).

Hexafluorophosphate (2,4,6-Tri-*tert*-butylphenyl)[bis(dimethylamino)methylidene]phosphanyl Radical Cation (**4**). In a Schlenck tube, 75 mg (0.2 mmol) of **1** and 66 mg (0.2 mmol) of hexafluorophosphate ferrocenium were dissolved in 1 mL of acetonitrile. The solution became deep violet immediately. The solvent was removed in vacuo to give a violet solid, which was washed twice with 5 mL portions of dry ether to remove

all traces of ferrocene. UV-vis (THF, nm): 255, 371.1 ($\epsilon = 5.4 \times 10^4$, $555.9 (2.1 \times 10^4)$, 760.

(2,4,6-Tri-tert-butylphenyl)[(dimethylamino)ethyl]phosphane²⁰ (**2**). In a dry Schlenck tube, to 500 mg of Mes*PH₂ (1.8 mmol) was added dropwise 1.5 mL (10 mmol) of *N,N*-dimethylacetamide dimethyl acetal. After addition, the solution was stirred under nitrogen (100 °C for 5 days). The mixture was brought slowly to room temperature over a couple of hours. ³¹P NMR showed peaks corresponding to the desired product and Mes*PH₂ (approximately 1/3 ratio). The product was purified by chromatography on silica gel, with hexane/ether 1:1 as an eluant, to obtain a pure white powder. Yield: 210 mg, 34%. Melting point: 80 °C.

NMR (293 K): ³¹P (CDCl₃) δ 94.3; ¹H NMR (CDCl₃) δ 1.24 (s, 3H, Me), δ 1.32 (s, 9H, C_{para}-CMe₃), 1.55 (d, 18H, ⁵J(P-H) = 1.00, C_{ortho}-CMe₃), 3.05 (d, 6H, ⁴J(P-H) = 5.00, NMe₂), 7.39 (d, 2H, ⁴J(P-H) = 1.55, H_{aromatic}); ¹³C (CDCl₃) δ 21.50 (d, ²J(P-C) = 11.4, P=C-Me), 31.05 (s, C_{para}-CMe₃), 31.45 (s, C_{ortho}-CMe₃), 32.50 (d, ⁴J(P-C) = 7.90, C_{ortho}-CMe₃), 33.45 (s, C_{para}-CMe₃), 38.40 (s, NMe₂), 42.05 (d, ³J(P-C) = 18.50, NMe₂), 121.30 (s, C_{meta}), 138.95 (d, ¹J(P-C) = 62.50, C_{ipso}), 148.90 (s, C_{para}), 155.50 (s, C_{ortho}), 189.20 (d, ¹J(P-C) = 62.10, P=C). HRMS: calculated for ¹²C₂₂¹H₃₈¹⁴N³¹P 347.27414, measured 347.27098.

Acknowledgment. We gratefully acknowledge support from Swiss National Science Foundation. P.R. thanks the portuguese Fundação da Ciência e Tecnologia for financing part of his post-doctoral fellowship.

Supporting Information Available: Crystal data, intensity measurement and structure refinement, atomic coordinates, displacement parameters, bond distances, and bond angles for **1a** (PDF); X-ray crystallographic file (CIF). Representation of the SOMO for **M1**⁺. This material is available free of charge via the Internet at <http://pubs.acs.org>.

References and Notes

- (1) Dillon, K. B.; Mathey, F.; Nixon, J. F. *Phosphorus: the Carbon Copy*; Wiley & Sons: Chichester, U.K., 1998.
- (2) *Multiple Bonds and Low Coordination in Phosphorus Chemistry*; Regitz, M.; Scherer, O. J., Eds.; Georg Thieme Verlag: Stuttgart, 1990.
- (3) (a) Geoffroy, M.; Jouaiti, A.; Terron, G.; Cattani-Lorente, M.; Ellinger, Y. *J. Phys. Chem.* **1992**, *96*, 8241. (b) Jouaiti, A.; Geoffroy, M.; Terron, G.; Bernardinelli, G. *J. Am. Chem. Soc.* **1995**, *117*, 2251. (c) Al Badri, A.; Jouaiti, A.; Geoffroy, M. *Magn. Reson. Chem.* **1999**, *37*, 735.
- (4) (a) Fuchs, E.; Breit, B.; Heydt, H.; Schoeller, W.; Busch, T.; Kruger, C.; Betz, P.; Regitz, M. *Chem. Ber.* **1991**, *124*, 2843. (b) Fuchs, E. P. O.; Heydt, H.; Regitz, M.; Schoeller, W. W.; Busch, T. *Tetrahedron Lett.* **1989**, *20*, 5111.
- (5) (a) Grobe, J.; Le Van, D.; Nientiedt, J.; Krebs, B.; Dartmann, M. *Chem. Ber.* **1988**, *121*, 655. (b) Grobe, J.; Le Van, D.; Krebs, B.; Frölich, R.; Schiemann, A. *J. Organomet. Chem.* **1990**, *389*, C29-C33. (c) Grobe, J.; Le Van, D.; Lange, G. *Z. Naturforsch. B* **1993**, *48*, 58.
- (6) Weber, L.; Uthmann, S.; Stamm, H.-G.; Neumann, B.; Schoeller, W. W.; Boese, R.; Blaser, D. *Eur. J. Inorg. Chem.* **1999**, 2369.
- (7) Frison, G.; Sevin, A. *J. Phys. Chem. A* **1999**, *103*, 10998.
- (8) Frison, G.; Sevin, A. *J. Organomet. Chem.* **2002**, *643-644*, 105-111.
- (9) For a review about phosphaalkenes with inverse electron density: Weber, L. *Eur. J. Inorg. Chem.* **2000**, 2425.
- (10) Arduengo, A. J., III; Carmalt, C. J.; Clybume, J. A. C.; Cowley, A. H.; Pyati, R. *Chem. Commun.* **1997**, 981.
- (11) Schoeller, W. W.; Niemann, J.; Thiele, R.; Hang, W. *Chem. Ber.* **1991**, *124*, 417.
- (12) Oehme, H.; Leissring, E.; Meyer, H. *Tetrahedron Lett.* **1980**, *21*, 1141.
- (13) Oehme, H.; Leissring, E.; Meyer, H. *Z. Chem.* **1981**, *21*, 407.
- (14) Appel, R.; Knoll, F.; Ruppert, I. *Angew. Chem., Int. Ed. Engl.* **1981**, *20*, 731.

(15) Crystal data for **1a**: (C₂₃H₄₃N₂O₂P) (H₂O); *M*_r = 426.6; $\mu = 0.13 \text{ mm}^{-1}$, $d_x = 1.123 \text{ g}\cdot\text{cm}^{-3}$, monoclinic, *P*2₁/*c*, *Z* = 4, *a* = 17.2208(12), *b* = 11.3657(6), *c* = 13.3749(10) Å, $\beta = 105.475(8)^\circ$, *V* = 2522.9(3) Å³. Data were collected at 200 K on a Stoe IPDS diffractometer. *R* = 0.039, ωR = 0.038, *S* = 1.26(2) for 2526 contributing reflections and 274 variables. Additional details are given as Supporting Information.

(16) Schmidpeter, A.; Zirzow, K.-H.; Willhalm, A.; Holmes, J. M.; Day, R. O.; Holmes, R. R. *Angew. Chem., Int. Ed. Engl.* **1986**, *25*, 457; *Angew. Chem., Int. Ed. Engl.* **1986**, *25*, 457.

(17) Weber, L.; Uthmann, S.; Stamm, H.-G.; Neumann, B.; Schoeller, W. W.; Boese, R.; Bläser, D. *Eur. J. Inorg. Chem.* **1999**, 1369.

(18) Navech, J.; Majoral, J. P.; Kraemer, R. *Tetrahedron Lett.* **1983**, *52*, 5885.

(19) Navech, J.; Revel, M.; Kraemer, R. *Phosphorus Sulfur* **1984**, *21*, 105.

(20) In contrast to refs 19 and 20, **2** was not found to be an oil, but a crystalline compound (mp = 80 °C).

(21) Soulié, E.; Berclaz, T.; Geoffroy, M. In *AIP Conference Proceedings 330*; Bernardi, F., Rivail, J.-L., Eds.; Computers and Chemistry; 1996; p 627.

(22) *WinEPR Simfonia, vJ.25*, Bruker Analytische Messtechnik GmbH, 1996.

(23) Rotation barriers *V* have been calculated (B3LYP/6-31+G(d)) as the electronic energy difference between the optimized structure and a nonoptimized structure where P-H or CH₂ has been rotated by 90°. See: Schmidt, M. W.; Truong, P. N.; Gordon, M. S. *J. Am. Chem. Soc.* **1987**, *109*, 5217.

(24) Arduengo, A. J., III; Rasika Dias, H. V.; Calabrese, J. C. *Chem. Lett.* **1997**, 143-44.

(25) Arduengo, A. J., III; Calabrese, J. C.; Cowley, A. H.; Rasika Dias, H. V.; Goerlich, J. R.; Marshall, W. J.; Riegel, R. *Inorg. Chem.* **1997**, *36*, 2151.

(26) Joantéguy, S.; Pfister-Guillouso, G.; Chermette, H. *J. Phys. Chem. A* **1999**, *103*, 350.

(27) Ohno, K.; Okamura, K.; Yamakado, H.; Hoshino, S.; Takami, T.; Yamauchi, M. *J. Phys. Chem.* **1995**, *99*, 14247.

(28) Lias, S. G.; Bartmess, J. E.; Liebman, J. F.; Holmes, J. L.; Levin, R. D.; Mallard, W. G. *J. Phys. Chem. Ref. Data* **1988**, *17* (Suppl. No. 1).

(29) Lacombe, S.; Gonbeau, D.; Cabioch, J.-L.; Pellerin, B.; Denis, J.-M.; Pfister-Guillouso, G. *J. Am. Chem. Soc.* **1998**, *110*, 6964.

(30) Voyna, V. I.; Alekseiko, L. N.; Okhota, B. V.; Ruban, A. V.; Romanenko, V. D.; Markovskii, L. N. *J. Gen. Chem. USSR (Engl. Transl.)* **1991**, *61*, 463.

(31) Chernega, A. N.; Antipin, M. Y.; Struchkov, Y. T.; Sarina, T. V.; Romanenko, V. D. *J. Struct. Chem.* **1986**, *27*, 741.

(32) Nguyen, M. T.; Creve, S.; Eriksson, L. A.; Vanquickenbome, L. G. *Mol. Phys.* **1997**, *91*, 537.

(33) Sidorenkova, H. Ph.D. Thesis, University of Geneva, Switzerland, 2001.

(34) Cramer, C. J.; Lim, M. H. *J. Phys. Chem.* **1994**, *98*, 5024.

(35) Kutzelnigg, W.; Fleischer, U.; Schindler, M. *NMR-Basic Principles and Progress*; Springer-Verlag: Heidelberg, 1991; Vol. 23, p 167.

(36) Godbout, N.; Salahub, D. R.; Andzelm, J.; Wimmer, E. *Can. J. Chem.* **1992**, *70*, 560.

(37) Glendingen, E. D.; Reed, A. E.; Carpenter, J. E.; Weinhold, F. *Natural Bond Orbital Analysis, NBO 3.1*; Theoretical Chemistry Institute, University of Wisconsin, Madison, WI. Calculations performed at the B3LYP/6-31+G(d) level.

(38) (a) Chentit, M.; Sidorenkova, H.; Jouaiti, A.; Terron, G.; Geoffroy, M.; Ellinger, Y. *J. Chem. Soc., Perkin Trans. 2* **1997**, 921. (b) Alberti, A.; Benaglia, M.; D'Angelantonio, M.; Emmi, S. S.; Guerra, M.; Hudson, A.; Macciantelli, D.; Paolucci, F.; Roffia, S. *J. Chem. Soc., Perkin Trans. 2* **1999**, 309.

(39) From a comparison with atomic coupling constants reported in: Morton, J. R.; Preston, K. F. *J. Magn. Reson.* **1978**, *30*, 577.

(40) (a) Cetinkaya, B.; Hudson, A.; Lappert, M. F.; Goldwhite, H. *J. Chem. Soc., Chem. Commun.* **1982**, 609. (b) Geoffroy, M.; Lucken, E. A. C.; Mazeline, C. *Mol. Phys.* **1974**, *28*, 839. (c) Kajita, M.; Endo, Y.; Hirota, E. *J. Mol. Spectr.* **1987**, *124*, 66. (d) Bonnazzola, L.; Michaut, J. P.; Roncin, J. *J. Chem. Phys.* **1981**, *75*, 4829. (e) Nelson, W.; Jackel, G.; Gordy, W. *J. Chem. Phys.* **1970**, *52*, 4572. (f) Fullam, B. W.; Mishra, S. P.; Symons, M. C. R. *J. Chem. Soc., Dalton Trans.*, **1974**, 2145. (g) Berclaz, T.; Geoffroy, M. *Helv. Chim. Acta* **1978**, *61*, 684.

(41) A representation of the SOMO for (HP=CH₂)⁺ (**M1**⁺) is given as Supporting Information.

(42) Frisch, M. J.; Trucks, G. W.; Schlegel, H. B.; Scuseria, G. E.; Robb, M. A.; Cheeseman, J. R.; Zakrzewski, V. G.; Montgomery, J. A.; Stratmann, R. E.; Burant, J. C.; Dapprich, S.; Millam, J. M.; Daniels, A. D.; Kudin, K. N.; Strain, M. C.; Farkas, O.; Tomasi, J.; Barone, V.; Cossi, M.; Cammi, R.; Mennucci, B.; Pomelli, C.; Adamo, C.; Clifford, S.; Ochterski, J.; Petersson, G. A.; Ayala, P. Y.; Cui, Q.; Morokuma, K.; Malick, D. K.; Rabuck, A. D.; Raghavachari, K.; Foresman, J. B.; Cioslowski, J.; Ortiz, J. V.; Stefanov, B. B.; Liu, G.; Liashenko, A.; Piskorz, P.; Komaromi, I.;

Gomperts, R.; Martin, R. L.; Fox, D. J.; Keith, T.; Al-Laham, M. A.; Peng, C. Y.; Nanayakkara, A.; Gonzalez, C.; Challacombe, M.; Gill, P. M. W.; Johnson, B. G.; Chen, W.; Wong, M. W.; Andres, J. L.; Head-Gordon, M.; Replogle, E. S.; Pople, J. A. *Gaussian 98*, Revision A.7; Gaussian, Inc.: Pittsburgh, PA, 1998.

- (43) Becke, A. D. *J. Chem. Phys.* **1993**, *98*, 5648.
(44) Lee, C.; Yang, W.; Parr, R. G. *Phys. Rev. B*, **1988**, *37*, 785.
(45) Wong, M. W. *Chem. Phys. Lett.* **1996**, *256*, 391.
(46) Reed, A. E.; Curtis, L. A.; Weinhold, F. *Chem. Rev.* **1988**, *88*, 899.
(47) P. F. Flukiger, Development of the molecular graphics package MOLEKEL and its application to selected problems in organic and organometallic chemistry, Thèse No. 2561, Département de chimie physique, Université de Genève, Genève, 1992.
(48) Portmann, S.; Luthi, H. P. *Chimia* **2000**, *54*, 766.

- (49) Widauer, C.; Shiahuy Chen, G.; Grützmacher, H. *Chem. Eur. J.* **1998**, *4*, 1154.
(50) DeFrees, D. J.; McLean, A. D. *J. Comput. Chem.* **1986**, *3*, 321.
(51) Barone, V. In *Recent Advances in Density Functional Methods, Part I*; Chong, D. P., Ed.; World Scientific Publishing Co.: Singapore, 1996.
(52) Rega, N.; Cossi, M.; Barone, V. *J. Chem. Phys.* **1996**, *105*, 11060.
(53) Barone, V. *Chem. Phys. Lett.* **1996**, *262*, 201.
(54) Yoshifuji, M.; Toyota, K.; Shibayama, K.; Inamoto, N. *Chem. Lett.* **1983**, 1653.
(55) Cowley, A. H.; Kilduff, J. E.; Newman, T. H.; Pakulski, M. *J. Am. Chem. Soc.* **1982**, *104*, 5820.
(56) Meerwein, H.; Florian, W.; Schön, N.; Stopp, G. *J. Liebigs Ann. Chem.* **1961**, *641*, 1.
(57) Johnstone, R. A. W.; Rose, M. E. *Tetrahedron* **1979**, *35*, 2169.